Pergamon

Available online at www.sciencedirect.com
SCIENCE DIRECT®

Cement and Concrete Research 33 (2003) 1741–1748

CEMENT AND CONCRETE RESEARCH

The solubility of selenate-AFt ($3CaO{\cdot}Al_2O_3{\cdot}3CaSeO_4{\cdot}37.5H_2O$) and selenate-AFm ($3CaO{\cdot}Al_2O_3{\cdot}CaSeO_4{\cdot}xH_2O$)

Isabel Baur*, C. Annette Johnson

Swiss Federal Institute for Environmental Science and Technology (EAWAG), Box 611, Dubendorf CH-8600, Switzerland

Received 18 September 2002; accepted 16 April 2003

Abstract

The Se(VI)-analogues of ettringite and monosulfate, selenate-AFt ($3CaO{\cdot}Al_2O_3{\cdot}3CaSeO_4{\cdot}37.5H_2O$), and selenate-AFm ($3CaO{\cdot}Al_2O_3{\cdot}CaSeO_4{\cdot}xH_2O$) were synthesised and characterised by bulk chemical analysis and X-ray diffraction. Their solubility products were determined from a series of batch and resuspension experiments conducted at 25 °C. For selenate-AFt suspensions, the pH varied between 11.37 and 11.61, and a solubility product, $\log K_{so} = 61.29 \pm 0.60$ ($I = 0$ M), was determined for the reaction $3CaO{\cdot}Al_2O_3{\cdot}3CaSeO_4{\cdot}37.5H_2O + 12\ H^+ \Longleftrightarrow 6Ca^{2+} + 2Al^{3+} + 3SeO_4^{2-} + 43.5H_2O$. Selenate-AFm synthesis resulted in the uptake of Na, which was leached during equilibration and resuspension. For the pH range of 11.75 to 11.90, a solubility product, $\log K_{so} = 73.40 \pm 0.22$ ($I = 0$ M), was determined for the reaction $3CaO{\cdot}Al_2O_3{\cdot}CaSeO_4{\cdot}xH_2O + 12\ H^+ \Longleftrightarrow 4Ca^{2+} + 2Al^{3+} + SeO_4^{2-} + (x+6)H_2O$. Thermodynamic modelling suggested that both selenate-AFt and selenate-AFm are stable in the cementitious matrix; and that in a cement limited in sulfate, selenate concentration may be limited by selenate-AFm to below the millimolar range above pH 12.

Keywords: Characterisation; Ettringite; Monosulfate; Modelling; Waste management

1. Introduction

The crystalline calcium sulfoaluminate hydrates, ettringite ($3CaO{\cdot}Al_2O_3{\cdot}3CaSO_4{\cdot}32H_2O$, an AFt phase, column-like structure), and monosulfate ($3CaO{\cdot}Al_2O_3{\cdot}CaSO_4{\cdot}12H_2O$, an AFm phase, lamellar structure) are formed during cement hydration. Ettringite is a product of the early hydration stage. Depending on the cement composition and the availability of CO_3^{2-}, ettringite either persists or is converted to monosulfate [1].

Both calcium sulfoaluminate hydrates have the ability to combine with a number of cations and anions, which makes them important with regard to waste immobilisation in cementitious matrices. Sulfate-substituted ettringites have been reported and synthesised for AsO_4^{3-}, $B(OH)_4^-$, CO_3^{2-}, CrO_4^{2-}, NO^{3-}, OH^-, SeO_4^{2-}, SO_3^{2-}, and VO_4^{3-} [2–6]. In the AFm phase, $B(OH)_4^-$, CrO_4^{2-}, MoO_4^{2-}, SeO_4^{2-}, and SO_3^{2-} may serve as interlayer anions [7–10]. Substitution of Se oxyanions is of particular interest because in nuclear waste management, Se is considered to have a high priority in the safety assessment [11].

Under oxygenated conditions, the oxyanionic species selenite (SeO_3^{2-}) and selenate (SeO_4^{2-}) are the predominant forms of Se. There is evidence to suggest that both selenite and selenate are stable in the cement matrix [12]. Selenite generally sorbs more strongly than selenate, this being attributed to its binding via inner-sphere complexes. Under acidic conditions, selenate may also form inner-sphere complexes. However, at high pH (>10), as found in cementitious systems, both selenite and selenate reach a sorption minimum [13–15]. In a previous study, the sorption of selenite and selenate to cement minerals was investigated [16]. It was found that selenite sorption was approximately the same for calcium silicate hydrate (C-S-H), ettringite, and monosulfate. The distribution ratios, R_d, found (0.18 to 0.38 $m^3\ kg^{-1}$) were similar to those determined previously for different cement formulations [17]. It was suggested that selenite was sorbed by surface complexation, until, at elevated selenite additions, $CaSeO_3$ was precipitated [16]. Substitution of sulfate by selenite in ettringite and monosulfate might have occurred, but it is quantitatively unimportant. Selenate showed a quite different behaviour. Its sorption on C-S-H and ettringite was only weak (R_d values were found to be <0.01 and 0.03 $m^3\ kg^{-1}$, respectively). In contrast, when selenate was added

* Corresponding author.
E-mail address: kellerbaur@freesurf.ch (I. Baur).

0008-8846/$ – see front matter © 2003 Published by Elsevier Ltd.
doi:10.1016/S0008-8846(03)00151-0

to monosulfate suspensions, 80% of the added selenate was sorbed within minutes ($R_d = 2$). X-ray diffraction analysis indicated a change in monosulfate interlayer distances with increasing selenate additions. In parallel, an increasing amount of ettringite was found in the sample. This led to the suggestion that selenate substituted for sulfate in monosulfate, while the exchanged sulfate precipitated in ettringite. To the knowledge of the authors, fully selenate substituted monosulfate (selenate-AFm) has not been described in the literature. In contrast, fully selenate substituted ettringite (selenate-AFt) has been synthesised and characterised before [18]. However, no thermodynamic data are available.

The purpose of this study was to synthesise and characterise the selenate analogue of monosulfate (selenate-AFm) and to determine its solubility product. In addition, the solubility product of selenate-AFt was established. Thermodynamic modelling with the obtained values was performed in order to assess the importance of the calcium aluminium selenate hydrates in the immobilisation of selenate in cementitious systems containing sulfate.

2. Experimental

2.1. Materials

All chemicals were at least of p.a. grade. To prevent a CO_2 contamination, all handling of material, the sampling, and the pH measurements were undertaken in a glovebox (Mecaplex) equipped with a CO_2 scrubber ($p_{CO2} < 1$ ppm, DMP). Solutions were prepared using boiled ultrapure water (millipore). Low-density polyethylene bottles and HDPE-centrifuge tubes were leached with acid (~ 0.1 M diluted from concentrated HNO_3) for at least 24 h and rinsed with ultrapure water three times. The same procedure, but with a more diluted HNO_3 solution ($\sim$pH 4), was used to leach and rinse 0.45 μm nylon filters (Whatman).

2.2. Mineral synthesis

In a first attempt, selenate-AFt was synthesised by mixing a CaO suspension with a solution containing stoichiometric amounts of $Na_2O{\cdot}Al_2O_3$ and Na_2SeO_4. This method is also called the "paste reaction" and can be used to prepare pure sulfate-AFt [19]. However, the resulting solid could not be identified as selenate-AFt. Another method used to prepare AFt phases is the "saccharate method," which involves a lime–sucrose complex [18]. It has been shown before that the paste reaction and the saccharate method can result in differently shaped crystals [4], and that sulfite-AFt could only be synthesised using the saccharate method [20]. In consequence, selenate-AFt was prepared successfully according to the saccharate method from stoichiometric amounts of $Na_2O{\cdot}Al_2O_3$ and Na_2SeO_4 (3.66 and 12.66 g, respectively, dissolved in 40 ml H_2O) and freshly burnt CaO (7.5 g dissolved in 0.5 l of a 10% sucrose solution). The mixture was stirred for 48 h and then left at room temperature. After 16 days, the solution was decanted and the solid was washed three times with ultrapure water to remove saccharate and sodium. The suspension was then filtered on a glass filter funnel. When the water suction was complete, acetone was filled into the funnel mixed with the solid and sucked off. This procedure was repeated three times.

For the synthesis of selenate-AFm, stoichiometric amounts of freshly burnt CaO (6.72 g) were mixed with $Na_2O.Al_2O_3$ (4.92 g) and Na_2SeO_4 (5.67 g) and cooled to 5 °C. Ultrapure water (200 ml, likewise cooled at 5°C) was added and the mixture was shaken for 24 h on a rotary shaker (150 rpm) at 5 °C. Afterwards, the suspension was cured for 5 1/2 months at room temperature. The solid was then centrifuged for 5 min at 8000 rpm and the solution decanted. The washing and drying procedures were the same as for selenate ettringite. The air-dried solids ($p_{CO2} < 1$ ppm) were stored in a dessicator over silica gel and soda lime. The size fraction < 0.125 mm was used for the determination of the solubility product.

2.3. Solid phase characterisation

The composition of the synthesised mineral was determined in duplicate by dissolving a portion (0.05 g) solid of the synthesised minerals solid in 50 g ultrapure water and 500 μl 65% HNO_3 and analysing the resultant solution. The total H_2O content of the solids was determined by thermogravimetry (Mettler Toledo Star System, 10 °C min^{-1} to 1000 °C) and by loss on ignition (LOI) at 850 °C for 4 h. Prior to weighing, the solids were equilibrated in a desiccator with a saturated $CaCl_2$ solution to maintain a relative humidity of approximately 30%. X-ray, powder diffraction was performed with a Scintag XDS 2000 diffractometer (Cu-Kα-radiation).

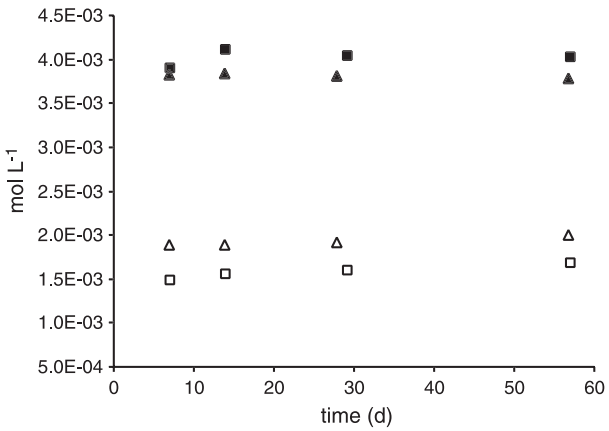

Fig. 1. Concentrations of Ca^{2+} (filled symbols) and SeO_4^{2-} (open symbols) in solution as a function of time in suspensions of selenate-AFm (squares) and selenate-AFt (triangles) at LS 250.

Table 1
Stability and solubility constants for dissolved species used in calculations for $I = 0$ M and $T = 25$ °C

Equilibrium reaction	log K_{SO}	Reference
$H_2O \Longleftrightarrow OH^- + H^+$	− 14.00	Ref. [30]
$Ca^{2+} + H_2O \Longleftrightarrow CaOH^+ + H^+$	− 12.70	Ref. [31]
$Al^{3+} + H_2O \Longleftrightarrow Al(OH)^{2+} + H^+$	− 4.97	Ref. [30]
$Al^{3+} + 2H_2O \Longleftrightarrow Al(OH)_2^+ + 2H^+$	− 9.30	Ref. [30]
$Al^{3+} + 3H_2O \Longleftrightarrow Al(OH)_3 + 3H^+$	− 15.00	Ref. [30]
$Al^{3+} + 4H_2O \Longleftrightarrow Al(OH)_4^- + 4H^+$	− 23.00	Ref. [30]
$SeO_4^{2-} + H^+ \Longleftrightarrow HSeO_4^-$	1.80	Ref. [32]
$SeO_4^{2-} + Ca^{2+} \Longleftrightarrow CaSeO_4$	2.00	Ref. [32]
Solid phases		
$3CaO{\cdot}Al_2O_3{\cdot}3CaSO_4{\cdot}32H_2O + 12H^+ \Longleftrightarrow 6Ca^{2+} + 2Al^{3+} + 3SO_4^{2-} + 38H_2O$	57.45	Ref. [26]
$3CaO{\cdot}Al_2O_3{\cdot}3CaSeO_4{\cdot}37.5H_2O + 12\ H^+ \Longleftrightarrow 6Ca^{2+} + 2Al^{3+} + 3SeO_4^{2-} + 43.5H_2O$	61.29	this study
$3CaO{\cdot}Al_2O_3{\cdot}CaSeO_4{\cdot}xH_2O + 12\ H^+ \Longleftrightarrow 4Ca^{2+} + 2Al^{3+} + SeO_4^{2-} + (x+6)H_2O$	73.40	this study

2.4. Determination of solubility product

For all equilibration experiments, 0.1 g solid was suspended in 25 ml of ultrapure water and equilibrated at 25 °C on a rotary shaker at 150 rpm. To determine the equilibration time, duplicate samples were equilibrated for 7, 14, 28, and 57 days. The samples were filtered through 0.45 μm nylon filters. The filter cakes were air dried ($p_{CO2} < 1$ ppm) and stored in a desiccator containing silica gel and soda lime. Equilibrium was achieved between 7 and 14 days (Fig. 1). In consequence, a set of 10 samples of each solid was equilibrated in parallel for 14 days. An additional set of 10 samples for each solid was obtained from supersaturated solutions by storing the samples at 40 °C for 7 days followed by a 14-day equilibration at 25 °C on a rotary shaker.

Repeated resuspension experiments were performed with both solids to check whether or not interconversions were occurring and to determine the congruency of dissolution. Five batches were performed in parallel for each solid by suspending 1.5 g in 25 ml ultrapure water in 50 ml HDPE centrifuge tubes. After a 10-day equilibration time at 25 °C on a rotary shaker (125 rpm), the solid was centrifuged down (20 min, 8000 rpm) and the supernatant was decanted for analysis (Cycle 0). The solids were resuspended in 25 ml ultrapure water and again equilibrated for 12 days. This procedure was repeated three times (Cycles 1 to 3, with equilibration times 10, 11, and 10 days, respectively). The amount of solid dissolved after four cycles had previously been estimated to be 10% at maximum. For solid phase characterisation, an additional sample for each resuspension step was prepared with 0.5 g solid in 5 ml ultrapure water of which the supernatant was discarded and the solids air dried ($p_{CO2} < 1$ ppm) for analysis.

The elemental composition of the resuspended selenate-AFm phase and of the equilibrated solids was determined by dissolving 0.015 g in a solution of 15 ml ultrapure water and 150 μl 65% HNO_3 and analysing resultant solution composition.

2.5. Sample analysis

The solution pH was measured at 25 °C in an unfiltered 10-ml aliquot using a combined glass electrode (Metrohm 6.0202.100) calibrated by an acid-based titration. The standard deviation of the measurement between pH 11 and 12 was 0.005. For the analysis of Na, Se, Ca, and Al, the filtered sample was acidified with 1% (v/v) of 65% HNO_3. The filtrates were stored in polyethylene bottles prior to analysis. Selenium was analysed by atomic absorption spectroscopy (Perkin Elmer 5100, standard deviation of the measurement < 5%) using the flame technique. Sodium,

Table 2
Elemental composition of the synthetic selenate-AFt and AFm

	Ca	Al	SeO_4	Na	H_2O	No. of replicates
Selenate-AFt						
Theoretical	6	2	3			
Ref. [18]	6	2.03	2.79		32	
In solid	6	1.82 ± 0.04	2.80 ± 0.09		37.7[a]/37.3[b]	2
Selenate-AFm						
Theoretical	4	2	1	–		
m_0	4	1.66 ± 0.07	0.99 ± 0.05	0.37 ± 0.02	13.3[a]/14.0[b]	2
m_{eq}	4	1.87 ± 0.07	0.97 ± 0.04	< 0.1		2
m_{re0}	4	1.71 ± 0.07	1.07 ± 0.04	0.22 ± 0.01		2
m_{re1}	4	1.81 ± 0.07	1.05 ± 0.04	< 0.1		2
m_{re2}	4	1.82 ± 0.07	1.10 ± 0.04	< 0.1		2
m_{re3}	4	1.82 ± 0.07	1.10 ± 0.04	< 0.1		2

The data are normalised to 6 mol of Ca for AFt and to 4 mol of Ca for AFm. The H_2O content is calculated assuming the determined composition. The initially synthesised solid is termed m_0. The m_{eq} represents the sample equilibrated for 14 days at LS 250. The m_{re0}–m_{re3} represents the samples equilibrated and resuspended zero to three times at LS 17. The uncertainty indicates the twofold standard deviation of the measurements.

[a] Determined by LOI.

[b] Determined by thermogravimetry.

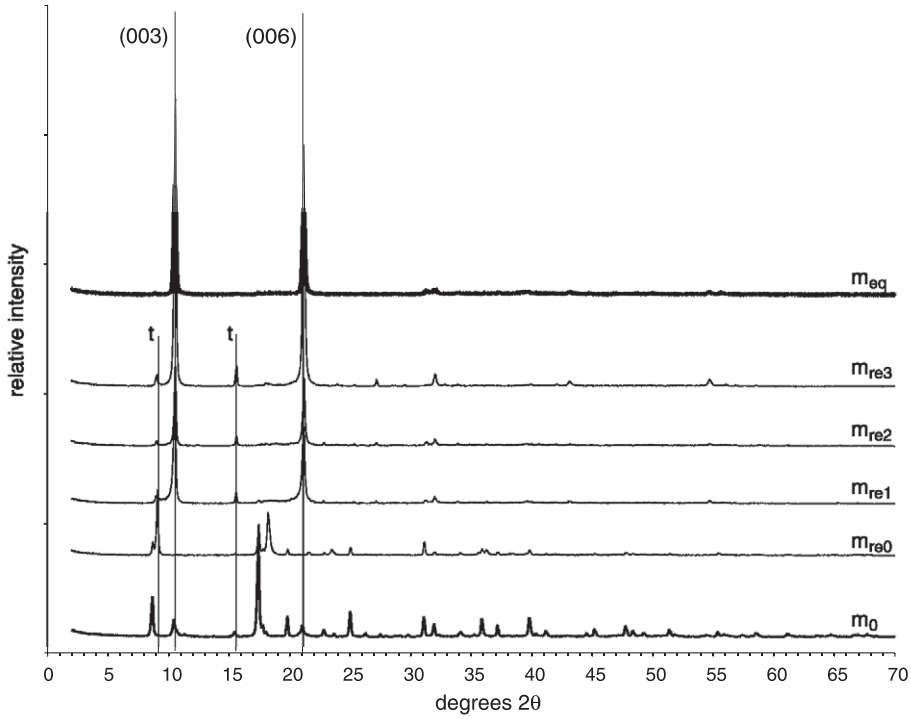

Fig. 2. XRD spectra of initially synthesised selenate-AFm (m_0) compared to the spectra derived from the repeated resuspension experiment (m_{re0}: equilibrated at LS 17; $m_{re1}-m_{re3}$: resuspended one to three times) and to the spectrum of selenate-AFm equilibrated at LS 250 (m_{eq}). The *hkl* (003) and (006) peak positions for $m_{re1}-m_{re3}$ and m_{eq} are pointed out with vertical lines. The vertical lines marked with t represent selenate-AFt peaks.

Ca, and Al concentrations were measured by inductively coupled plasma–optical emission spectroscopy (Spectroflame, Spectro Analytical Instruments, standard deviation of the measurement $<0.5\%$).

2.6. Calculation of solubility products

Speciation and thermodynamic equilibrium calculations were performed with the aid of the computer program MQV40TIT [21] based on MICROQL by Westall [22]. Thermodynamic data used for calculations are given in Table 1. They were adjusted for the ionic strength of the solution using the Davies equation.

3. Results and discussion

3.1. Characterisation of the synthesised minerals

The XRD spectrum of the synthesised selenate-AFt agrees with the powder diffraction file (PDF) 42-0224 in the database of the International Center for Diffraction Data (ICDD), which represents $3CaO{\cdot}Al_2O_3{\cdot}3CaSeO_4{\cdot}32H_2O$. No change in the spectrum could be observed in equilibrated samples at liquid to solid ratio (LS) 250 and 17 and in samples resuspended at LS 17 between one and three times.

The elemental composition of the synthesised selenate-AFt is given in Table 2. Compared to the theoretical composition, the synthesised selenate-AFt contained less aluminate and selenate. This indicates that there is either a deficiency of Al and Se or an excess of Ca. It is difficult to explain this observation in terms of AFt column stoichiometry. It is more likely, particularly in view of the similar Ca excess in the AFm phase, that the elemental measurements were precise but not sufficiently accurate. It is also possible that additional Ca phases, such as portlandite, are present at quantities below about 5% w/w, which would not be detectable by XRD. In addition to this, the water content of the synthesised selenate-AFt was high at 37.5 in comparison to published values (Ref. [18, p.32]. However, the observed stoichiometric divergence of the theoretical composition does not affect the crystal structure, as shown by XRD. The excess in water is possibly weakly bound water located in the interchannels [23].

Table 3
Determined layer distance of initially synthesised selenate-AFm (m_0), at LS ratio 17 equilibrated selenate-AFm (m_{re0}), one to three times resuspended selenate-AFm ($m_{re1}-m_{re3}$), and at LS 250 equilibrated selenate-AFm (m_{eq}), see also Fig. 2

Solid phase	Layer distance (nm)	Reference
m_0	1.02	this study
m_{re0}	0.975/1.02	this study
$m_{re1}-m_{re3}$	0.84	this study
m_{eq}	0.84	this study
U phase	1.002	PDF 44-0272
Cr(VI)-AFm	0.8402	PDF 42-0063

For comparison, the layer distance of U phase ($4CaO{\cdot}Al_2O_3{\cdot}1.5SO_3{\cdot}0.5Na_2O{\cdot}15H_2O$) and Cr(VI)-AFm ($Ca_4Al_2O_6(CrO_4){\cdot}9H_2O$) is given.

Table 4
XRD data for the at LS 250 equilibrated sample (m_{eq})

°2θ	d (Å)	Int
10.50	8.415[a]	100
21.12	7.922	2
31.30	5.116	1
31.91	5.075	2
31.17	4.203[b]	77
21.62	4.107	2
39.48	4.081	2
43.01	2.867	3
21.76	2.855	4
54.53	2.838	2
11.16	2.802[c]	4
31.50	2.413	1
17.46	2.291	1
17.32	2.281	2
44.68	2.263	1
39.30	2.101	2
39.80	2.026	1
37.24	1.681	2

Int denotes relative peak intensity.
[a] *hkl* 003.
[b] *hkl* 006.
[c] *hkl* 009.

Normalised to four Ca, the synthesised selenate-AFm contained 0.84 Al_2O_3, 0.99 SeO_4, 0.37 NaO, and 14 H_2O per formula unit (Table 2). During equilibration and resuspension, Na was leached from the solids. In the sample equilibrated at LS 250 (m_{eq}) and in the sample resuspended one to three times at LS 17 (m_{re1}–m_{re3}), the Na content decreased to <0.1 mol per formula unit. The decrease of Na content was accompanied by an increase in aluminium content, approaching the theoretical AFm composition. It is known that monosulfate synthesised in the presence of high Na concentrations incorporates Na in the AFm structure. The so-called U phase, $4CaO{\cdot}0.9Al_2O_3{\cdot}1.1SO_3{\cdot}0.5Na_2O{\cdot}16H_2O$, is then precipitated [24,25]. It is possible that a similar uptake occurs in selenate-AFm.

The XRD spectra obtained for freshly synthesised selenate-AFm (m_0) differed strongly from the 14 days equilibrated (m_{eq}) and the resuspended samples (Fig. 2). The differences can be interpreted by the difference in Na content. The AFm-layer distance, c', represented by the Miller indices, *hkl* 003 and 006 in Fig. 2, decreases in parallel with the decreasing Na content. The layer distances for the different samples are given in Table 3. Unfortunately, no reference XRD spectrum is known for selenate-AFm, but the layer distance of the U phase and our Na-containing selenate-AFm is in good agreement. Also, the layer distances of our samples in which the Na has been washed out are close to those of chromate-AFm. Sodium ions may have a repulsive effect on the Ca–Al sheets, thus resulting in an increase in interlayer distance. A change in water content may also be the reason for the change in interlayer distances and it is possible that an increased Na content leads to an increase in water content. In the case of monosulfate, e.g., the number of water molecules per formula unit can vary between 8 and 16, which corresponds to c' values between 0.79 and 1.03 nm [1]. However, since all samples were dried under the same conditions, the observed change of c' seems more probably to be caused by changes in the Na content. Unfortunately the water content of the equilibrated and resuspended samples could not be determined because of the small quantities of material recovered.

The peaks observed at 9 and 15.6 °2θ found in the spectra of the samples resuspended at LS ratio 17, m_{re1}, m_{re2}, and m_{re3} can be attributed to selenate-AFt (Fig. 2). This indicates that interconversion from selenate-AFm to selenate-AFt has occurred to some extent.

Considering these findings, it can be concluded that the spectrum obtained for the sample m_{eq} corresponds to the

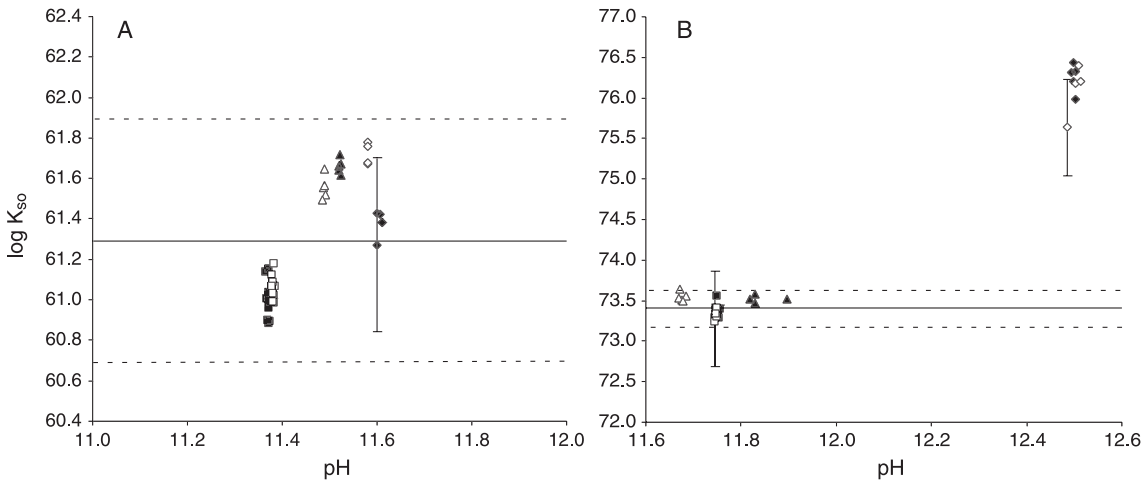

Fig. 3. Solubility products (log K_{so}) determined for selenate-AFt (A) and selenate-AFm (B) under different conditions. The squares indicate data points obtained from solids equilibrated at LS 250 for 14 days at 25 °C (■) and equilibrated for 7 days at 40 °C followed by 14 days at 25 °C (□). The diamonds and triangles represent data points from the resuspension experiment (LS 17, 25 °C) with (◆) equilibrated, (◇) resuspended once, (▲) resuspended twice, and (△) resuspended three times. The error bars represent the twofold standard deviation of the measurement valid for all samples. The horizontal lines denote the average log K_{so} value with the dashed lines denoting their twofold standard deviation (in B, the data sets ◆ and ◇ were excluded, see text).

Table 5
Solubility products (K_{SO}) of the calcium aluminate selenate hydrates corrected to ionic strength, $I = 0$ M

Mineral	I (M)	log K_{SO}	No. of replicates
Selenate-AFt			
14 days at 25 °C, LS 250	0.012	61.00 ± 0.14	10
7 days at 40 °C, then 14 days at 25 °C, LS 250	0.012	61.05 ± 0.14	10
re0 (12 days at 25 °C, LS 17)	0.012	61.38 ± 0.19	5
re1 (10 days at 25 °C, LS 17)	0.012	61.72 ± 0.22	4
re2 (11 days at 25 °C, LS 17)	0.012	61.66 ± 0.19	5
re3 (10 days at 25 °C, LS 17)	0.012	61.56 ± 0.19	5
Average value		61.29 ± 0.60	39
Selenate-AFm			
14 days at 25 °C, LS 250	0.015	73.36 ± 0.19	10
7 days at 40 °C, then 14 days at 25 °C, LS 250	0.015	73.33 ± 0.19	10
re0 (12 days at 25 °C, LS 17)	0.065	(76.25 ± 0.26)	5
re1 (10 days at 25 °C, LS 17)	0.048	(76.10 ± 0.30)	4
re2 (11 days at 25 °C, LS 17)	0.015	73.52 ± 0.30	4
re3 (10 days at 25 °C, LS 17)	0.013	73.55 ± 0.26	5
Average value		73.40 ± 0.22	29

The experimental conditions, including the ionic strength, under which the determinations were carried out are also listed. Values in brackets are not included in the average value. The abbreviation re0 to re3 denote the samples equilibrated and resuspended zero to three times.

pure selenate-AFm, $3CaO{\cdot}Al_2O_3{\cdot}CaSeO_4{\cdot}xH_2O$, with a layer distance of 0.84 nm (Table 4). This spectrum agrees well with the spectrum for chromate-AFm ($3CaO{\cdot}Al_2O_3{\cdot}CaCrO_4{\cdot}9H_2O$, PDF 42-0063) with the same layer distance. However, the water content of the equilibrated selenate-AFm remains unknown.

3.2. Solubility products

Solubility products were calculated for solutions of the experiments in which equilibration was achieved from both under- and supersaturation at LS 250 and for the solutions of the repeated resuspension experiment at LS 17. The solubility products have been formulated according to the following reactions:

$$3CaO{\cdot}Al_2O_3{\cdot}3CaSeO_4{\cdot}37.5H_2O + 12H^+ \Longleftrightarrow 6Ca^{2+} + 2Al^{3+} + 3SeO_4^{2-} + 43.5H_2O$$

$$K_{SO} = \frac{[Ca^{2+}]^6[Al^{3+}]^2[SeO_4^{2-}]^3}{[H]^{12}} \quad (1)$$

and

$$3CaO{\cdot}Al_2O_3{\cdot}CaSeO_4{\cdot}xH_2O + 12H^+ \Longleftrightarrow 4Ca^{2+} + 2Al^{3+} + SeO_4^{2-} + (6+x)H_2O$$

$$K_{SO} = \frac{[Ca^{2+}]^4[Al^{3+}]^2[SeO_4^{2-}]}{[H]^{12}} \quad (2)$$

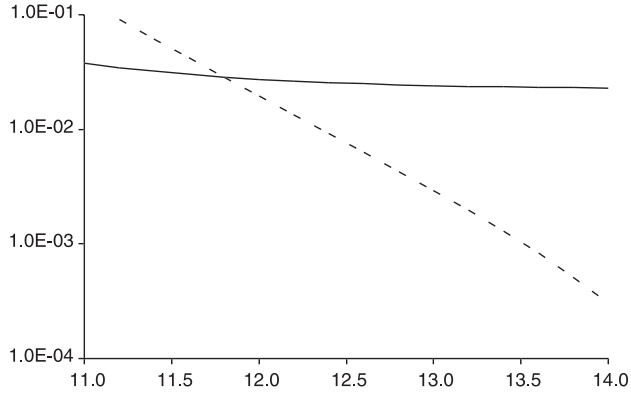

Fig. 4. Modelled selenate solubility against pH in the presence of ettringite and selenate-AFt (solid line) and ettringite and selenate-AFm (dashed line) with sulfate activity set to 10^{-3} mol l^{-1}.

For selenate-AFt, the solubility products determined under different conditions and coming from under- and supersaturation agree well (Fig. 3). The average value calculated for all experiments is log $K_{so} = 61.29 \pm 0.60$ (Table 5). For the sake of comparison, solubility products for AFt phases reported for ettringite (e.g., Ref. [26]) and for Cr(VI)-AFt [6] have values ($I = 0$, 25 °C) of 57.45 and 60.54, respectively.

In the case of selenate-AFm, the solubility products derived from the samples m_{re0} and m_{re1} of the resuspension experiment are significantly higher than the other values (Fig. 3 and Table 5). In these samples, the pH was also substantially higher because of the high Na content in the batches. It is likely that the solid solution formation between pure selenate-AFm and sodium-selenate-AFm affected the solubility of selenate-AFm. In consequence, the high values obtained from samples m_{re0} and m_{re1} were not included. The average value for log K_{so} is 73.40 ± 0.22 for selenate-AFm. The respective solubility products for monosulfate and chromate-AFm are 72.57 [26] and 71.62 [10].

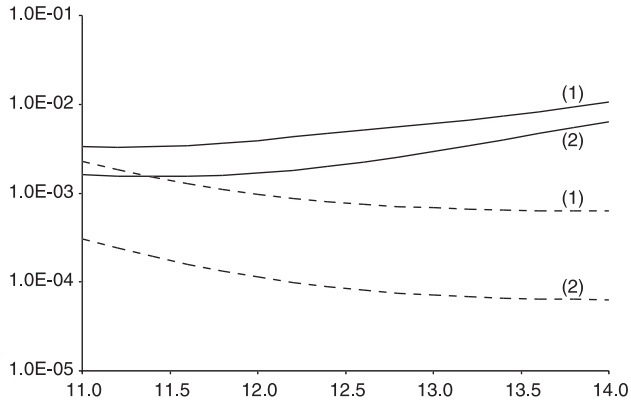

Fig. 5. Modelled selenate solubility against pH in the presence of monosulfate and selenate-AFt (solid lines) and monosulfate and selenate-AFm (dashed lines) with sulfate activity set to 10^{-4} mol l^{-1} (1) and 10^{-5} mol l^{-1} (2).

The determined solubility products were used to model the selenate solubility within cementitious material when controlled by selenate-AFt and selenate-AFm. For modelling, ordinary Portland cement pore water compositions were applied ($SO_4 = 10^{-3}$ mol l^{-1}, $I = 0.5$ M [27]). Stability and solubility constants were adjusted using Pitzer according to Millero and Schreiber [28]. Because no Pitzer coefficients for Se(VI) are known, Cr(VI) constants were applied to Se(VI) species. Selenate solubility was modelled either in the presence of ettringite or monosulfate. Both calcium aluminosulfate hydrates may control Al, Ca, and SO_4 solubilities in cementitious matrices, and therefore directly influence selenate-AFt and selenate-AFm solubility. Monosulfate is thermodynamically unstable with respect to ettringite in cements [26]; however, at low sulfate concentrations, monosulfate may be the more stable phase.

In Fig. 4, the solubility of selenate against pH in the presence of ettringite and selenate-AFt or selenate-AFm is illustrated. It is shown that above pH 12 selenate-AFm is the more stable phase. The dependency of the selenate-AFm stability on pH can explain the increased interconversion to selenate-AFt observed in the third resuspension sample where the solution pH was lowest at 11.68 (Figs. 2 and 3).

In order to test the influence of sulfate limitation in cement pore water on selenate solubility, monosulfate was chosen as the Al- and Ca-controlling phase, and sulfate activity was set to 10^{-4} mol l^{-1} and 10^{-5} mol l^{-1}. Such low sulfate concentrations can occur in the pore waters of high-alumina cements [29]. The dependency of varying sulfate concentration on selenate solubility in the presence of monosulfate and selenate-AFt or selenate-AFm is shown in Fig. 5. For both selenate-AFt and selenate-AFm, the selenate solubility decreases with decreasing sulfate concentration. In the case of selenate-AFm, this decrease is more distinct and comprises one order of magnitude. This scenario illustrates that selenate-AFm may limit selenate concentrations to below the millimolar range when the system is limited in sulfate. However, any later addition of sulfate to the system will increase the selenate solubility when ettringite becomes predominant.

Nevertheless, the solubilities of selenate-AFm and selenate-AFt are relatively similar indicating that both solids may be stable in a cementitious system. The predominance of either AFm or AFt phases seems difficult do predict, as it is also the case for the sulfate analogues ettringite and monosulfate. Further studies need to elucidate the boundary conditions favouring AFm or AFt structure in the presence of different anions.

Acknowledgements

The authors gratefully acknowledge the funding of the Swiss Federal Institute of Environmental Science and Technology (EAWAG). Günther Kahr (ETH Zürich) is kindly acknowledged for thermogravimetric analyses.

References

[1] H.F.W. Taylor, Cement Chemistry, Thomas Telford, London, 1997.
[2] P. Kumarathasan, G.J. McCarthy, D.J. Hassett, D.F. Pflughoeft-Hasset, Oxyanion substituted ettringites: synthesis and characterization; and their potential role in immobilization of As, B, Cr, Se and V, Mater. Res. Soc. Symp. Proc. 178 (1990) 83–104.
[3] G.J. McCarthy, D.J. Hassett, J.A. Bender, Synthesis, crystal chemistry and stability of ettringite, a material with potential applications in hazardous waste immobilization, Mater. Res. Soc. Symp. Proc. 245 (1992) 129–140.
[4] H. Pöllmann, S. Auer, H.-J. Kuzel, Solid solution of ettringites: Part II. Incorporation of $B(OH)_4^-$ and CrO_4^{2-} in $3CaO{\cdot}Al_2O_3{\cdot}3CaSO_4{\cdot}32H_2O$, Cem. Concr. Res. 23 (1993) 422–430.
[5] S.C.B. Myneni, S.J. Traina, T.J. Logan, G.A. Waychunas, Oxyanion behavior in alkaline environments: sorption and desorption of arsenate in ettringite, Environ. Sci. Technol. 31 (1997) 1761–1768.
[6] R.B. Perkins, C.D. Palmer, Solubility of $Ca_6[Al(OH)_6]_2(CrO_4)_3{\cdot}26H_2O$, the chromate analog of ettringite; 5–75 °C, Appl. Geochem. 15 (2000) 1203–1218.
[7] A. Kindness, E.E. Lachowski, A.K. Minocha, F.P. Glasser, Immobilisation and fixation of molybdenum (VI) by Portland cement, Waste Manage. 14 (1994) 97–102.
[8] H. Motzet, H. Pöllmann, Synthesis and characterisation of sulfite-containing AFm phases in the system $CaO\text{-}Al_2O_3\text{-}SO_2\text{-}H_2O$, Cem. Concr. Res. 29 (1999) 1005–1011.
[9] M. Zhang, Incorporation of oxyanionic B, Cr, Mo, and Se into hydrocalumite and ettringite: application to cementitious systems, PhD thesis, University of Waterloo, Canada, 2000.
[10] R.B. Perkins, C.D. Palmer, Solubility of chromate hydrocalumite ($3CaO{\cdot}Al_2O_3{\cdot}CaCrO_4{\cdot}nH_2O$) 5–75 °C, Cem. Concr. Res. 31 (2001) 983–992.
[11] S. Kemakta, A.B. Konsult, Modelling of water flow, barrier degradation, chemistry and radionuclide transport in the near field of a repository for L/ILW, Technical report NTB 88-42, Nagra, 1989.
[12] I. Bonhoure, I. Baur, C.A. Johnson, E. Wieland, A.M. Scheidegger, Se(IV/VI) immobilization by cementitious systems: an X-ray absorption study (in preparation).
[13] K.F. Hayes, A.L. Roe, G.E. Brown Jr., K.O. Hodgson, J.O. Leckie, G.A. Parks, In situ X-ray absorption study of surface complexes: selenium oxyanions on a-FeOOH, Science 238 (1987) 783–786.
[14] R.P.J.J. Rietra, T. Hiemstra, W.H.V. Riemsdijk, Comparison of selenate and sulfate adsorption on goethite, J. Colloid Interface Sci. 240 (2001) 384–390.
[15] D. Peak, D.L. Sparks, Mechanisms of selenate adsorption on iron oxides and hydroxides, Environ. Sci. Technol. 36 (2002) 1460–1466.
[16] I. Baur, C.A. Johnson, Sorption of selenite and selenate to cement minerals, Environ. Sci. Technol (accepted for publication).
[17] E.A. Johnson, M.J. Rudin, S.M. Steinberg, W.H. Johnson, The sorption of selenite on various cement formulations, Waste Manage. 20 (2000) 509–516.
[18] D.J. Hassett, G.J. McCarthy, P. Kumarathasan, D. Pflughoeft-Hassett, Synthesis and characterization of selenate and sulfate–selenate ettringite structure phases, Mater. Res. Bull. 25 (1990) 1347–1354.
[19] M. Atkins, D. Macphee, A. Kindness, F.P. Glasser, Solubility properties of ternary and quaternary compounds in the $CaO\text{-}Al_2O_3\text{-}SO_3\text{-}H_2O$ system, Cem. Concr. Res. 21 (1991) 991–998.
[20] H. Pöllmann, Die Kristallchemie der Neubildungen bei Einwirkung von Schadstoffen auf hydraulische Bindemittel, PhD thesis, Friedrich-Alexander University, Erlangen, Germany, 1984.
[21] G. Furrer, Version 4.0; Institute of Terrestrial Ecology (ITÖ), Schlieren, Switzerland, 1995.

[22] J.C.W. Westall, MICROQL: I. A chemical equilibrium program in Basic: II. Computation of adsorption equilibria in Basic, Technical report, EAWAG, 1979.
[23] H. Pöllmann, H.-J. Kuzel, R. Wenda, Compounds with ettringite structure, N. Jb. Miner. Abh. 160 (1989) 133–158.
[24] G. Li, P. LeBescop, M. Moranville, The U phase formation in cement-based systems containing high amounts of Na_2SO_4, Cem. Concr. Res. 26 (1996) 27–33.
[25] G. Li, P. LeBescop, M. MoranvilleRegourd, Synthesis of the U phase ($4CaO{\cdot}0.9Al_2O_3{\cdot}1.1SO_3{\cdot}0.5Na_2O{\cdot}16H_2O$), Cem. Concr. Res. 27 (1997) 7–13.
[26] D. Damidot, F.P. Glasser, Thermodynamic investigation of the CaO-Al_2O_3-$CaSO_4$-H_2O system at 25 °C, Cem. Concr. Res. 23 (1993) 221–238.
[27] E.E. Lachowski, F.P. Glasser, A. Kindness, K. Luke, in: H. Justnes (Ed.), 10th International Congress on the Chemistry of Cement, vol. 3, Amarkai and Congress Göteborg, Gothenburg, 1997, p. 3ii091.
[28] F.J. Millero, D.R. Schreiber, Use of ion pairing model to estimate activity coefficients of the ionic components of natural waters, Am. J. Sci. 282 (1982) 1508–1540.
[29] M. Ochs, B. Lothenbach, E. Giffaut, Uptake of oxo-anions by cements through solid-solution formation: experimental evidence and modelling, Radiochim. Acta 90 (2002) 639.
[30] C.F. Baes, R.E. Mesmer, The Hydrolysis of Cations, Wiley-Interscience, Malabar, FL, 1986, reprinted by Robert E. Krieger Publishing.
[31] R.M. Smith, A.E. Martell, Critical Stability Constants, Inorganic Complexes, vol. 4, Plenum, New York, 1976, pp. 1–12.
[32] F. Séby, M. Potin-Gautier, E. Giffaut, G. Borge, O.F.X. Donard, A critical review of thermodynamic data for selenium species at 25 °C, Chem. Geol. 171 (2001) 173–194.